Separation and Purification Technology 187 (2017) 118–126

Contents lists available at ScienceDirect

Separation and Purification Technology

journal homepage: www.elsevier.com/locate/seppur

Enhanced hydrophilicity and mechanical robustness of polysulfone nanofiber membranes by addition of polyethyleneimine and Al_2O_3 nanoparticles

Nigmet Uzal [a,*], Nuray Ates [b], Seda Saki [c], Y. Emre Bulbul [b], Yongsheng Chen [d]

[a] Department of Civil Engineering, Abdullah Gul University, Kayseri 38080, Turkey
[b] Department of Environmental Engineering, Erciyes University, Kayseri 38039, Turkey
[c] Advanced Materials and Nanotechnology, Abdullah Gul University, Kayseri 38080, Turkey
[d] School of Civil and Environmental Engineering, Georgia Institute of Technology, Atlanta, GA 30332, United States

ARTICLE INFO

Article history:
Received 3 October 2016
Received in revised form 14 June 2017
Accepted 19 June 2017
Available online 20 June 2017

Keywords:
Polysulfone nanofiber membrane
Polyethylenimine
Al_2O_3 nanoparticles
Electrospinning

ABSTRACT

A novel hydrophilic and mechanically robust polysulfone (PSF) nanofiber membrane (NFM) was prepared by electrospinning of a PSF solution blended with polyethyleneimine (PEI) and Al_2O_3 nanoparticles. The influence of PEI and Al_2O_3 nanoparticles concentration on the NFM characteristics was studied using scanning electron microscopy (SEM), Fourier transform infrared FT-IR spectroscopy, porosity, water contact angle measurement, and tensile strength test. Filtration performance of the nanofiber membranes (NFMs) were evaluated by the measurement of pure water flux (PWF) and bovine serum albumin (BSA) rejection tests. According to the results, blending PSF solution with 2 wt.% PEI and 0.05 wt.% Al_2O_3 nanoparticles resulted in formation of NFMs with high porosity and increased mechanical strength, which exhibited a low water contact angle of 23.5° and high water flux of 28,456 L/m^2 h. On the other hand, incorporation of nanoparticles and PEI in the PSF membrane matrix led to increasing of tensile strength that it was changed from 0.15 to 0.69 for pure PSF and PSF/PEI/Al_2O_3, respectively. A-24 and 48% BSA rejection performances were obtained by nanoparticle incorporated PSF membranes. In conclusion, the studies strongly suggest that blending with hydrophilic additives of NFMs can enhance the hydrophilicity and mechanical strength of PSF membranes and these NFMs can be effectively used in water based membrane systems.

© 2017 Elsevier B.V. All rights reserved.

1. Introduction

Nanofibers have recently attracted a great deal of attention in industry and academia due to their potential use in many applications such as protective clothing, advanced composites, sensors, tissue engineering, pharmaceutical industries and air filters [1–4]. Nanofibers also have a great potential in membrane filtration technology because of their high porosity, submicron pore sizes, and large surface area to volume ratio, which facilitates easily tailored membrane thickness and lower production costs [5–10]. Their promising structural properties make them good candidates for water based membrane filtration applications [11–13]. These NFMs have been shown to be effective at removing 1–10 μm size particulates [6,7] in aqueous solutions and, thus, can be used pretreatment for wastewater prior to the treatment by ultrafiltration (UF), nanofiltration (NF) and reverse osmosis (RO).

Different polymers are used as NFM materials such as polysulfone (PSF), polyvinylidene (PVDF) difluoride, polyacrylonitrile, cellulose acetate and polyether sulfone [14–20]. Among the polymers, PSF is widely used in preparing membranes because of its excellent properties such as chemical resistance, mechanical strength, and thermal stability [21,22]. Although there are some challenges in the application of PSF because of its hydrophobicity which can cause membrane fouling and low performance, easy manufacturing of membranes makes this polymer more desirable in water-based membrane filtration applications. Within this context, there is no option to have ideal engineering polymer having only advantage for fabricating membranes [23–25]. To overcome the disadvantages of polymers and enhance the membrane properties for high performance, many modifications have been made including incorporation of other materials such as nanoparticles (NPs) and hydrophilic polymers [18,26–28]. For example, many inorganic

* Corresponding author.
E-mail address: nigmet.uzal@agu.edu.tr (N. Uzal).

http://dx.doi.org/10.1016/j.seppur.2017.06.047
1383-5866/© 2017 Elsevier B.V. All rights reserved.

NPs, such as silica [29], titanium dioxide [30], zeolite [31], MWCNTs [32], ZrO_2 [33], ZnO [34], and Al_2O_3 [35–37], were incorporated into the polymeric matrices to generate hybrid membranes. Among these inorganic nanoparticles, Al_2O_3 have attracted much attention due to their availability, stability, hydrophilicity and suitable mechanical strength [35–38]. Studies show that the incorporation of Al_2O_3 results in enhanced hydrophilicity and mechanical strength [35,39,40].

Except for inorganic NPs, there are many hydrophilic polymers used as hydrophilic additives such as poly (ethylene glycol) (PEG) [36] and polyvinylpyrrolidone [40]. Polyethyleneimine (PEI) is a promising agent for the fabrication of high performance NFMs. In this respect, Park et al. [41] prepared PVDF nanofiber membranes using PEI as a hydrophilic agent for nanofiltration application and reported that PVDF nanofiber membranes became more hydrophilic than pure PVDF nanofiber membranes and showed high salt rejections.

The incorporation of NPs and hydrophilic agents in PSF membranes has been widely studied by other research groups; however, to the best of our knowledge, the effects of PEI-Al_2O_3 incorporation into PSF membranes have not yet been analyzed in detail. Therefore, this study focused on the preparation of hydrophilic and mechanically robust PSF nanofiber membranes by the addition of Al_2O_3 and PEI to the electrospinning solution. All membrane samples were characterized in terms of membrane morphology, average fiber diameter, porosity, chemical structure, water contact angle and mechanical strength. Pure water flux and bovine serum albumin (BSA) rejection potential of NFMs were evaluated with a dead-end filtration cell system. The results provide important insights into the effect of PEI and Al_2O_3 addition in polysulfone nanofiber membranes in terms of mechanical strength and hydrophilicity.

2. Experimental

2.1. Materials

PSF based polymer with a weight-average molecular weight of 60,000 was purchased from Acros Organics. Branched PEI aqueous solution with a number-average molecular weight of 10,000 and a weight-average molecular weight of 25,000 was obtained from Sigma-Aldrich used as a hydrophilic agent. N,N-dimethylformamide (Merck, anhydrous, 99.8%) and 1-methyl-2-pyrrolidinone (Merck) were used as the solvents. Hydrophilic Al_2O_3 particles with nano-size of 80 nm were used as additive for PSF-PEI polymer solutions and purchased from Nanografi (Turkey). BSA was obtained from Amresco Inc. (USA) having an average molecular weight of 66 kDa [42,43]. All of the organic and inorganic reagents were of analytical grade and used as received.

2.2. Membrane fabrication

2.2.1. Preparation of PSF/PEI-Al_2O_3 NFMs via electrospinning

The 25 wt.% PSF solution was prepared in a mixture of N,N-dimethylformamide and 1-methyl-2-pyrrolidinone at a ratio of 70:30, and different concentrations of PEI and Al_2O_3 NPs were added to the PSF solution. The mixture was stirred overnight with a magnetic stirrer to ensure the dissolution of the pellets and proper mixing. Final solution was ultrasonicated for two hours at a 40 kHz running speed to remove the air bubbles. The detailed polymer solution compositions and spinning parameters are summarized in Table 1.

The electrospinning apparatus was a Nanospinner Ne300 (Turkey). The polymeric solutions were held in a 10 ml plastic syringe, and the syringe needle was connected to a DC power supply. During electrospinning, the applied voltage and the distance of the needle tip to collector were 12.5 kV and 12 cm, respectively. During experiments, constant operational relative humidity and temperature were applied at 15–17% and 20–25 °C, respectively. The obtained membranes were stored during overnight at room conditions to remove the residual solvents.

2.3. Membrane characterization

2.3.1. Scanning electron microscope (SEM)

The morphological features of the fabricated NFMs were observed by SEM. The membrane samples were carefully sectioned with an approximate size of 3 mm length and 0.5 mm width using a sharp pair of scissors, and then mounted onto an SEM grid. Prior to the examination, each sample was coated with platinum using a JEOL JFC 1600 Autofine coater. A LEO 440 scanning electron microscope (Leica Zeiss, Germany) at 10 kV was used to analyze the samples. The average fiber diameter of each NFM was quantified from the SEM image using Digimizer by Softpedia. Measurements were performed at 50 random positions and the average of these measurements gave the diameter of the nanofibers.

2.3.2. Thickness and porosity

The thickness of NFMs in each sample was measured using a digital micrometer (No. 293-561, Mitutoyo, Japan) with ±0.1 μm accuracy. The average thickness of the NFMs at five different positions was adopted for the mean thickness of the NFMs and it also in mechanical strength calculations.

For the porosity measurements, the NFMs (dry weight, W_d) were immersed in isopropanol for three hours and the weights of NFMs soaked in isopropanol were recorded as W_1. Then, the liquid on the surface of the NFMs were removed by filter paper after being taken out from isopropanol. The weight of the wet NFMs was recorded as W_w. The porosity (ε) of the NFMs were calculated using in formula is given in Eq. (1):

$$\varepsilon = \frac{Ww - Wd}{Ww - W1} \times 100 \quad (1)$$

2.3.3. Water contact angle

In order to evaluate NFMs hydrophilicity, the water contact angle was measured by the sessile drop method at room temperature using Attension-Theta-Lite tensiometers (Biolin Scientific, Finland). A 5.0 μL pure water droplet was placed onto the NFM surface using a micro syringe. Distilled water was used to observe contact angle and compare it with the pure PSF, PSF/PEI and PSF/PEI-Al_2O_3 NFMs. For each contact angle measurement, at least three readings from different surface locations were conducted, and the average contact angles reported for each pure and modified membranes from measurements were calculated. All of the membranes were fully dried before measuring the contact angle to avoid water interaction issues.

2.3.4. FT-IR

Fourier transform infrared FT-IR spectroscopy measurements were employed to functional identification of PEI and Al_2O_3. FT-IR spectra of the NFMs were collected in the wave number range of 500–4000 cm^{-1} in transmission mode using a Thermo Nicolet Avatar 370 spectrometer. Prior to the FT-IR measurement, the samples were dried in a drying-oven for 15 min at 120 °C.

2.3.5. Mechanical strength

Mechanical strength of electrospinning NFMs were carried out with an AGS-J tensile testing machine (Shimadzu, Japan) according to the ASTM D 882 standard by applying a 500 N load cell at a crosshead speed of 1 mm/min. All the samples were cut into

Table 1
Fabrication of NFMs.

	Spinning solution composition			Electrospinning condition		
Membrane	PSF (wt.%)	PEI (wt.%)	Al_2O_3 (wt.%)	Flow rate (μL/h)	Applied voltage (kV)	Working distance (cm)
PSF	25	–	–	100	12.5	12
NFM 1	25	0.5	–	150	12.5	12
NFM 2	25	1	–	150	12.5	12
NFM 3	25	2	–	200	12.5	12
NFM 4	25	2	0.01	220	12.5	12
NFM 5	25	2	0.03	220	12.5	12
NFM 6	25	2	0.05	250	12.5	12

rectangles with dimensions of 6 × 2 cm^2 and vertically mounted in between two mechanical gripping units of the tester, leaving a 2 cm gauge length for mechanical loading. The sample thicknesses were measured with an electronic micrometer having a precision of ±0.1 μm.

2.3.6. Pure water flux

A dead-end system (Sterlitech, HP4750) was used to perform water filtration tests. The effective filtration area of the cell was 14.6 cm^2. The tested NFMs were placed in the filtration cell which was then filled with 250 ml of pure water. The filtration pressure was maintained by a compressed N_2. All the water filtration experiments were carried out at a stirring speed of 250 rpm and at 0.5 bar. The pure water flux J_w [L/(m^2 h)] was calculated by using Eq. (2);

$$Jw = \frac{V}{(A \cdot \Delta t)} \tag{2}$$

where V (L) is the volume of permeated water, A (m^2) is the membrane area, and Δt (h) is the permeation time.

2.3.7. BSA rejection

In order to evaluate the filtration performance of prepared NFMs, BSA solution with the concentration of 2.5 g/L was prepared at room temperature by dissolving a pre-weighed amount of BSA powder in distilled water. After pure water flux measurements, BSA rejection tests were conducted using dead-end stirred cell. Firstly, the BSA solution were scanned by a UV–Vis spectrophotometer (UV-1800, Shimadzu, China) between 200 nm and 800 nm. Then, the BSA concentrations in both feed and permeate were evaluated the absorbance at 280 nm [44,45] based on the UV scan. The BSA rejection, which indicated the separation performance of NFMs, was calculated from the concentrations of feed and permeate BSA solutions using the Eq. (3) [44]:

$$R = \left(1 - \frac{Cp}{Cf}\right) \times 100 \tag{3}$$

where C_f is the concentration of BSA in feed solution and C_p is the concentration of BSA in permeate solution.

3. Results and discussion

3.1. Morphological properties

One of the most important parameter in membrane characterization is the surface morphology of the membranes. Therefore, the membrane surface was observed by SEM from the microscale (PSF, PSF/PEI and PSF/PEI- Al_2O_3 NFMs Fig. 1a–e) to the nanoscale (PSF/PEI-Al_2O_3 NFMs Fig. 2a–c). Fig. 1a displays SEM images of the PSF NFMs. As shown, the NFMs obtained from the proper solution PSF concentration of 25 wt.% are smooth and beadless. The images of the NFM3, NFM4, NFM5 and NFM6 are demonstrated in Fig. 1b, c, d, e; as exhibited, the NFM loading by PEI and PEI/Al_2O_3 also showed beadless NFMs.

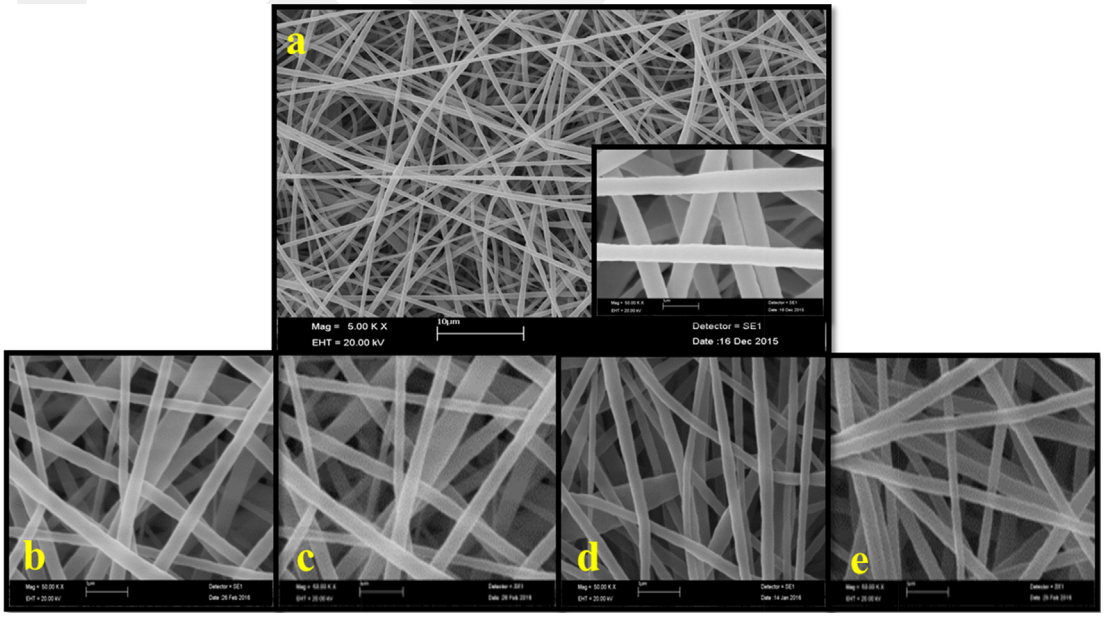

Fig. 1. SEM images of the PSF NFMs with respect to the PEI and Al_2O_3 concentration in the electrospinning solution: (a) PSF, (b) NFM3, (c) NFM4, (d) NFM5, (e) NFM6.

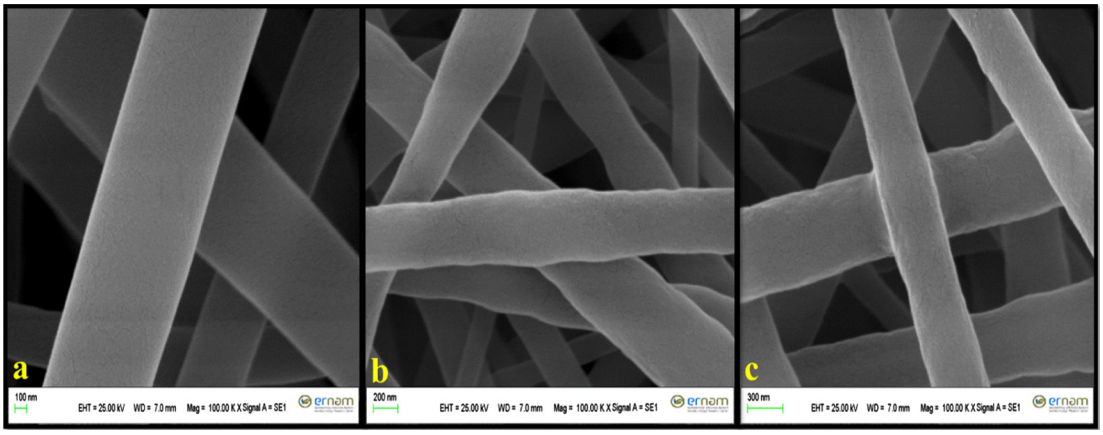

Fig. 2. Nanoscale SEM images of the NFMs with respect to the Al_2O_3 nanoparticles concentration in the electrospinning solution: (a) NFM4, (b) NFM5, (c) NFM6.

Table 2
Thickness, average fiber diameter and porosity of the NFMs.

Membrane	Thickness (mm)	Average fiber diameter (nm)	Porosity (%)
PSF	0.140 ± 0.05	672.3 ± 196.2	79.0
NFM 1	0.102 ± 0.01	406.7 ± 124.3	81.2
NFM 2	0.100 ± 0.01	381 ± 104.6	83.9
NFM 3	0.106 ± 0.03	308 ± 69.1	86.3
NFM 4	0.109 ± 0.02	418.4 ± 135.5	80.2
NFM 5	0.102 ± 0.01	354.7 ± 74.8	89.1
NFM 6	0.100 ± 0.02	304.4 ± 81.7	92.4

Table 3
Viscosity measurements of solutions used in membrane fabrication.

Membrane	Viscosity (cp)
PSF	1429
NFM 3	5258
NFM 4	6028
NFM 5	N/A*
NFM 6	10,291

* N/A: Not Applicable.

The PSF/PEI-Al_2O_3 NFMs are illustrated with nanometer scale in Fig. 2a, b and c. As displayed, the obtained nanofibers are decorated by Al_2O_3, which have uniform size. From these images, it can be concluded that the most of utilized Al_2O_3 were embedded inside the PSF nanofibers. It was reported that electrospinning of polymer, which is blending with NPs, leads to incorporation of the solid NPs inside the obtained nanofibers [46].

Furthermore, the observed diameters of PSF, PSF/PEI and PSF/PEI-Al_2O_3 nanofibers were analyzed using image analyzer software (ImageJ) to estimate the average diameter of the nanofibers and the results were given in Table 2.

The NFMs average fiber diameters were obviously reduced with increased PEI and Al_2O_3 concentrations from 0.5 wt.% to 2 wt.% and 0.01 wt.% to 0.05 wt.%, respectively. As shown in Table 2, the average fiber diameter of PSF was 672.3 ± 196.2 nm. After adding 2 wt.% of PEI into the spinning solution, the diameter of NFM slightly decreased with the average fiber diameter of 308 ± 69.1 nm. When the addition of Al_2O_3 was increased to 0.05 wt.%, the average fiber diameter was significantly reduced to 304.4 ± 81.7 nm. This was mainly due to the fact that the incorporation of PEI and Al_2O_3 could improve the conductivity and viscosity of the electrospinning solution, resulting in a decrease of the fiber diameter as determined by [46,47]. As shown in Table 3, the viscosity was increased from 1429 cp in pure PSF membrane to 10,291 cp in NFM6 membrane. Viscosity measurements of spinning solutions (Table 3) also proved that the increase in viscosity of solution resulted in thinner fiber diameters. Johan et al. [48] also reported that incorporation of Al_2O_3 as a nano-ceramic filler in polymer electrolytes solutions is ionic conductivity of the polymer electrolytes increases with increasing wt.% of Al_2O_3. In addition, incorporation of PEI and Al_2O_3 nanoparticles results higher porosity than PSF ones (Table 2).

The mentioned results about average fiber diameter variation, porosity and embedding of the nanoparticles might influence the mechanical and water contact angle (hydrophilicity) properties of the nanofiber membranes and thus could be of significant effects.

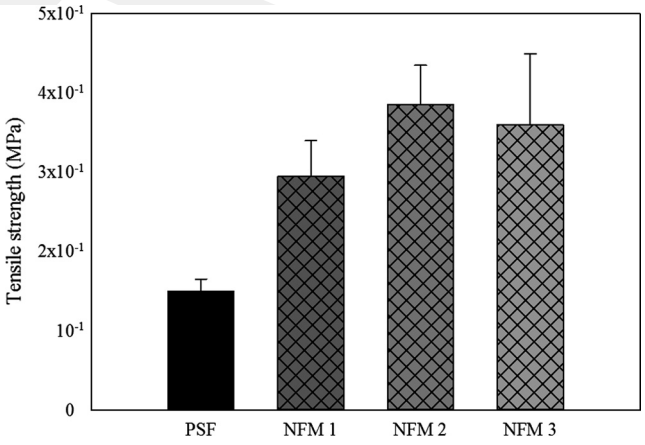

Fig. 3. Tensile strength of the NFMs in terms of the PEI concentration in the electrospinning solution: (PSF) 0 wt.% PEI, (NFM 1) 0.5 wt.% PEI, (NFM 2) 1 wt.% PEI, (NFM 3) 2 wt.% PEI.

3.2. Mechanical properties

The mechanical properties of NFMs with respect to the PEI and Al_2O_3 concentrations in terms of the tensile strength parameter were shown in Fig. 3. As shown in Fig. 3, the PEI content influences the tensile properties. The PSF NFM showed poor mechanical properties and the tensile strength was 0.15 MPa. The tensile strength of the NFMs evidently increases when the PEI and Al_2O_3 are incorporated in the PSF matrix 0.36 and 0.69, respectively. Comparing with the PSF membrane, the PSF/PEI and PSF/PEI-Al_2O_3 membranes had a slightly higher tensile strength. This could be explained by two aspects. On the one hand, the incorporation of PEI was favorable for the formation of the membrane matrix with branched chains, resulting in increase in the tensile strength of the nanofiber

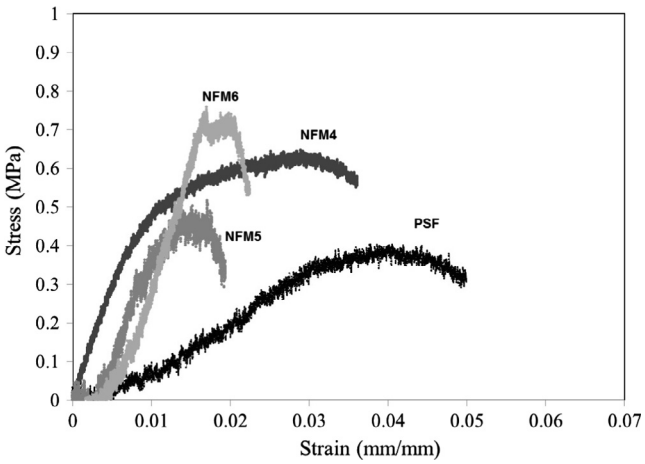

Fig. 4. Stress-strain curves of the NFMs in terms of the Al_2O_3 nanoparticles concentration in the electrospinning solution: (PSF) 0 wt.% Al_2O_3, (NFM 4) 0.01 wt.% Al_2O_3, (NFM 5) 0.03 wt.% Al_2O_3, (NFM 6) 0.05 wt.% Al_2O_3.

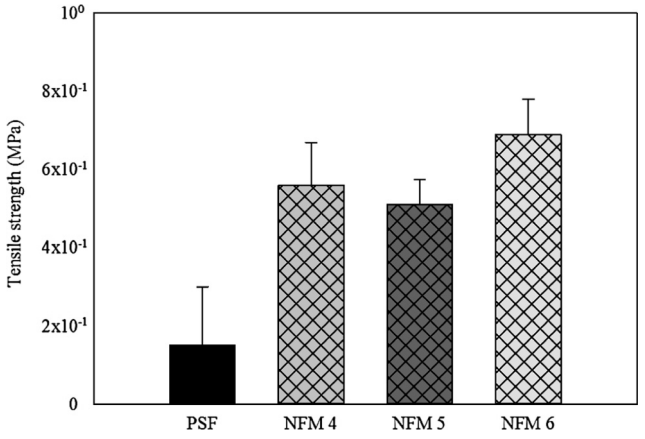

Fig. 5. Tensile strength of the NFMs in terms of the Al_2O_3 nanoparticles concentration in the electrospinning solution: (PSF) 0 wt.% Al_2O_3, (NFM 4) 0.01 wt.% Al_2O_3, (NFM 5) 0.03 wt.% Al_2O_3, (NFM 6) 0.05 wt.% Al_2O_3.

membranes. On the other hand, Al_2O_3 nanoparticles possess high mechanical strength, which could enhance the mechanical properties of the NFMs [36]. In the study of Yang et al. [49], quaternized poly(vinyl alcohol)/alumina (QPVA/Al_2O_3) polymer membrane was prepared by a solution casting method. Al_2O_3 fillers enhanced the mechanical properties of polymer in the presence of up to 10 wt. % of dispersed Al_2O_3. Similar results were also reported by Zhou et al. [50] and Zhang et al. [51] that Al_2O_3 composites presented higher mechanical properties when Al_2O_3 particles were blended with vinylend- blocked polymethylsiloxane or high density polyethylene.

The stress-strain curves of PSF/PEI-Al_2O_3 NFMs were given in Fig. 4. As the tensile strengths at breaking point were pointed out in Fig. 5, it is worth noting that the PSF/PEI-Al_2O_3 NFMs had the largest tensile strength. This could be due to the presence of PEI, which served as a coupling agent and significantly enhanced the compatibility between the polymer matrix (PSF) and inorganic filler Al_2O_3 [46,52]. The force exerted on the polymer matrix could be well transferred and consumed by the inorganic filler, resulting in superior tensile strength. As seen from Figs. 4 and 5, the highest tensile strength was obtained for 0.05 wt.% Al_2O_3 incorporated NFM.

The incorporation of PEI and Al_2O_3 to improve the tensile strength of NFMs is simple compared to previous studies including different methods and can achieve similar results compared with what other researchers have reported. Hou et al. [53] prepared PAN nanofibers containing multiwall carbon nanotubes (MWCNTs) by electrospinning a MWCNT and they found that MWCNTs reinforced the PAN nanofibers and improved the tensile strength by 75% at 5 wt.% MWCNTs. Ma et al. [54] applied heat treatment on PSF NFMs and there was a treble improvement on tensile strength. Huang et al. [55] increased the tensile strength of PSF NFM by 400% (0.8–3.2 MPa) via solvent treatment. In this work, PEI and Al_2O_3 incorporated in the PSF membrane matrix result in a similar nanofiber membranes with a relatively increase in tensile strength by 360% (0.1–0.6 MPa).

3.3. Water contact angle

In order to assess the relative hydrophilic/hydrophobic properties of the PSF/PEI-Al_2O_3 NFMs, water contact angle of NFMs were determined. In addition to the mechanical strength of PSF NFMs, hydrophilicity is another important parameter to be used for water based membrane filtration. The results showed that the PSF NFM exhibited a hydrophobic property with a WCA value of 119.75 ± 1.9. As can be seen in Fig. 6, the WCA values with 0.5 wt.%, 1 wt.% and 2 wt.% PEI addition in the PSF membrane matrix were found 101.33, 66.16 and 34.17, respectively. The reasons for this result were possibly attributed to the comprehensive influences of the strong hydrophilic characteristics of the PEI. Park et al. [41] also observed similar results on PVDF NFMs using PEI as a hydrophilic agent. Xu et al. [56] also reported that the contact angle values of composite electrospun membranes based on carbon nanotube network decreased as increasing the additive amount of MWCNTs and lower contact angle values showed an enhancement of the water flux of the composite membranes.

Water contact angle measurements which are given in Fig. 7 imply a higher hydrophilicity of the PSF/PEI-Al_2O_3 NFMs as compared to the pure PSF ones. The water contact angle of 34.17° for the NFM3 increased to 45.7° for NFM5. This could be because of a direct relationship between water contact angle and the average nanofiber diameter, which has been explained in detail by [47,52]. Obaid et al. [47] have reported that incorporation of silica NPs in the PSF nanofiber responsible about the observed small increase in water contact angle and this referred to the effect of nanofiber diameter on the liquid solid interface. They also attributed to the increase surface roughness of the nanofiber membranes. Generally, addition of metal nanoparticles such as Al_2O_3 is expected to do the hydrophobic membranes more hydrophilic. Because of low concentration NPs addition in the membrane matrix could not effect

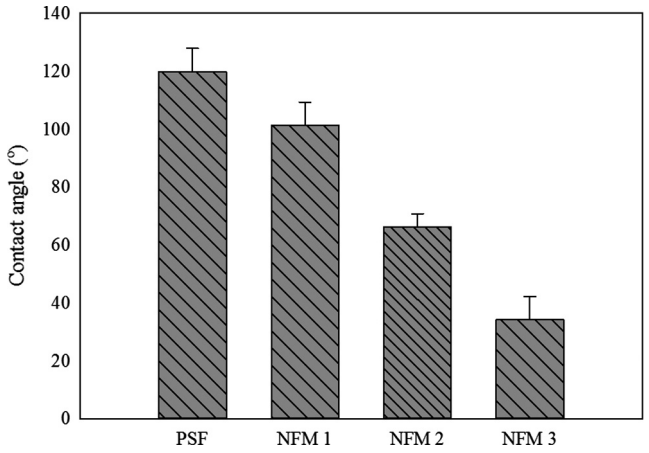

Fig. 6. Water contact angles of the NFMs with respect to the PEI concentration.

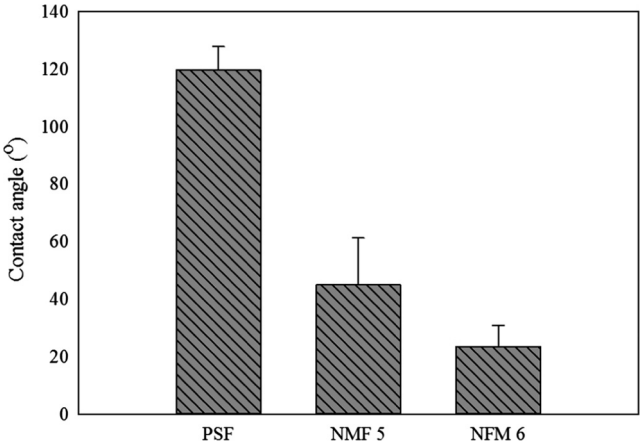

Fig. 7. Water contact angles of the NFMs with respect to the Al_2O_3 concentration.

of hydrophilicity. This is because, when NP content increases to 0.05 wt.%, the water contact angle of NFMs obviously decreased. Similarly, results can be attributed to the embedding of NPs into the PSF nanofibers and respect to obtained results, the nanoparticles is more beneficial in terms of tensile strength rather than hydrophilicity.

3.4. FT-IR analyses

The comparative FT-IR spectra of the PSF membrane, PSF/PEI and PSF/PEI-Al_2O_3 were given in Fig. 8. It could be found that the characteristic absorption peaks of PSF (Fig. 8) were at around 1149 cm^{-1} and 1168 cm^{-1} (SO_2 symmetrical stretch), 1244 cm^{-1} (Aryl-O-aryl C—O stretch), 1582 cm^{-1} (SO_2 asymmetric stretch), 1677 cm^{-1} (asymmetric–CH_3), and 2151 cm^{-1} (C═C) [57,58] and they were also presented in the spectra of the PSF/PEI and PSF/PEI- Al_2O_3 NFMs. This indicated that the structures of the PSF were well preserved. No additional peak was observed for the PSF/PEI NFMs because of the strongest bands of PEI overlapped with bands of PSF. In addition, the peak at 3730 cm^{-1} could be assigned to a C═O double bond, which was also a new peak for PSF/PEI- Al_2O_3 NFMs in agreement with the data given in [37,59].

3.5. Pure water flux

Water flux measurements were performed using a dead-end stirred cell and the pure water flux performances of the NFMs are shown in Fig. 9. It can be seen that the pure water permeability of all NFMs increased with PEI and Al_2O_3 loading. PSF NFMs exhibited minimum pure water flux of 14,268 L/m^2h because of its hydrophobic nature. Incorporation of 0.5, 1 and 2 wt.% PEI to the PSF NFM led to a gradual increase in the pure water flux to 19,726; 20,985 and 26,255, respectively, as a result of the increased membrane porosity and hydrophilicity [60]. Maximum pure water flux of 28,456 L/m^2 h was achieved by the NFMs from the solution containing 2 wt.% PEI and 0.05 wt.% Al_2O_3 nanoparticles. The reason is it's the highest porosity and the smallest contact angle as compared to the other NFMs. In addition, the high mechanical strength of NFM 6, which was previously proved by the tensile test, led to its lower compaction during the resultant high pure water flux. In comparison, Guclu et al. [61] have reported pure water flux of 1605 L/m^2 h under 0.2 bar for PSF/PAN NFM with PET nonwoven support layer while our all NFMs have a higher pure water flux. This could be a result of our preparation system did not have any support layer and our NFMs have lower thickness.

3.6. Evaluation of the BSA rejection

In the present research, the rejection performance of the PSF nanofiber membranes was assessed using 2.5 g/L BSA as a model foulant. The BSA rejection values for PSF, NFM1, NFM2 and NFM3, NFM4, NFM5 and NFM6 were calculated as 6.7%, 15.9%, 18.4% and 18.7%, 24.3%, 21.1% and 48.3%, respectively. The flux variations of the NFMs were evaluated to corroborate the rejection potential of the NFMs and to determine the effect of porosity, average fiber diameter and hydrophilicity on the rejection of the NFMs. With respect to Fig. 9, a remarkable value of PWF was obtained for all of the NFMs prepared in this study as a result of their high porosity and hydrophilicity [52]. As can be seen in Figs. 10 and 11, the BSA flux of the NFMs decreased as either 2.5 g/L BSA was passed over the NFM without an effective rejection. However, the observed highest rejection of NFM6 in comparison with the rejection of the other NFMs correlates with lower fiber diameter and higher hydrophilicity [60].

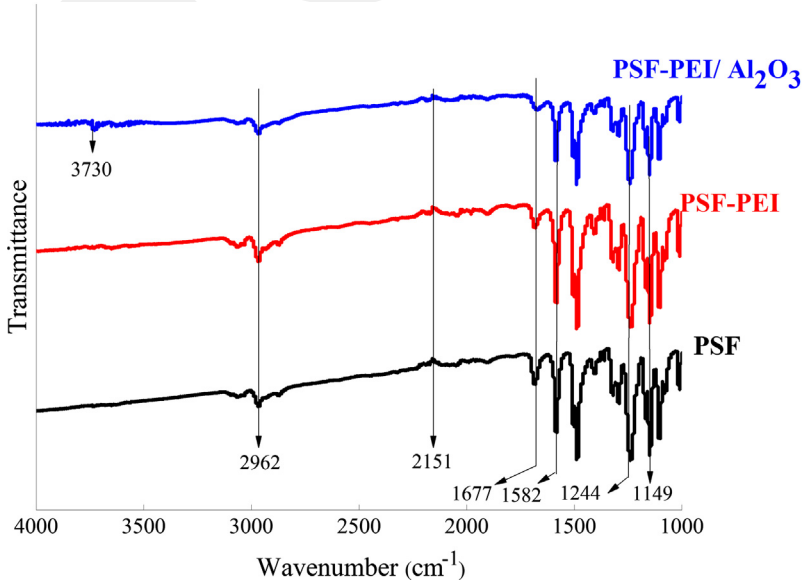

Fig. 8. FT-IR spectra of PSF, PSF/PEI and PSF/PEI-Al_2O_3 nanofiber membranes.

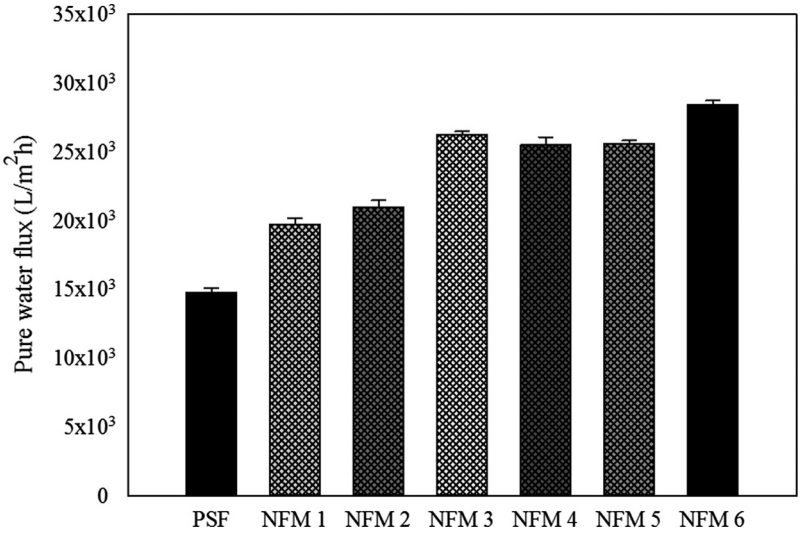

Fig. 9. Pure water flux performance of the NFMs.

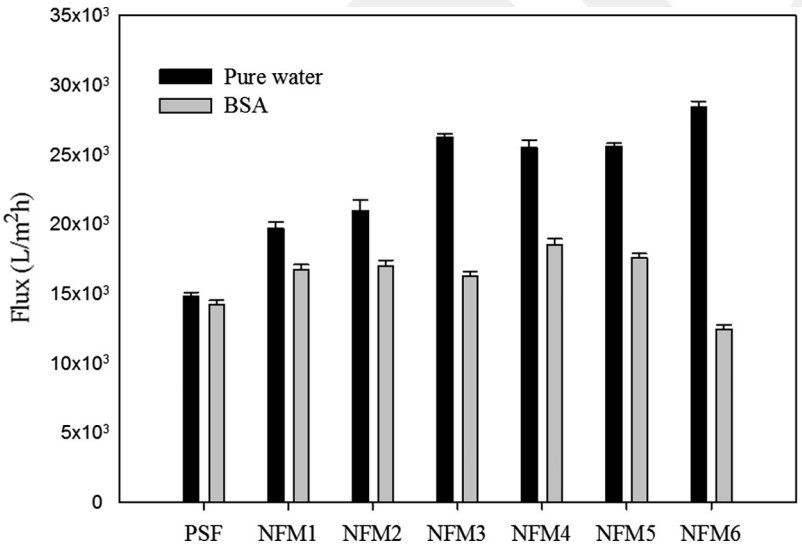

Fig. 10. Pure water and BSA flux performance of the NFMs.

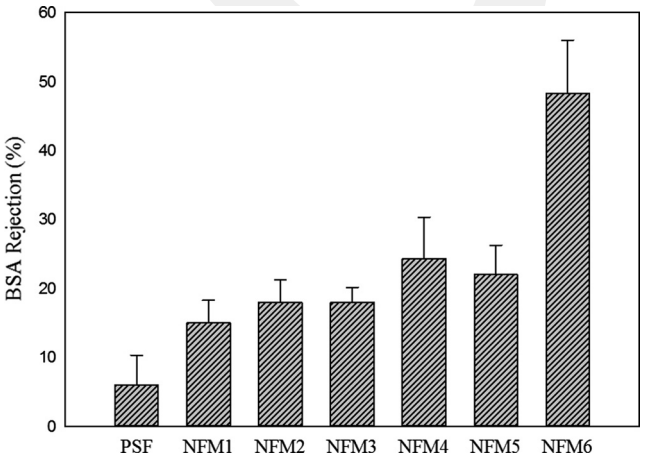

Fig. 11. BSA rejection performance of the NFMs.

The results showed the PSF/PEI-Al_2O_3 NFM were more efficient than the PSF NFM in the separation of BSA because the pure water flux and BSA rejection of the NFMs membranes are higher than the PSF membrane. This behavior can be related to the higher hydrophilicity of the PSF/PEI- Al_2O_3 as confirmed by the contact angle tests [60]. Furthermore, the study of Goetz et al. [62] indicated that filtration of BSA with CA nanofiber membrane showed higher BSA flux than our NFMs because of their higher hydrophilicity by referred 0° water contact angle. According to the results, the PEI and PEI/Al_2O_3 incorporated NFMs have higher pure water flux and BSA rejection than PSF membrane.

BSA compounds are used to evaluate the filtering performance of both MF and UF membranes [42,43,63,64]. In this study, the rejection performances of the PSF nanofiber membranes were assessed using 2.5 g/L BSA as a model foulant and the results showed that the BSA rejection values for NFM membranes were between 24 and 48% (Fig. 11). Based on the lower BSA rejection performances and the molecular weight of BSA (66 kDa) indicated

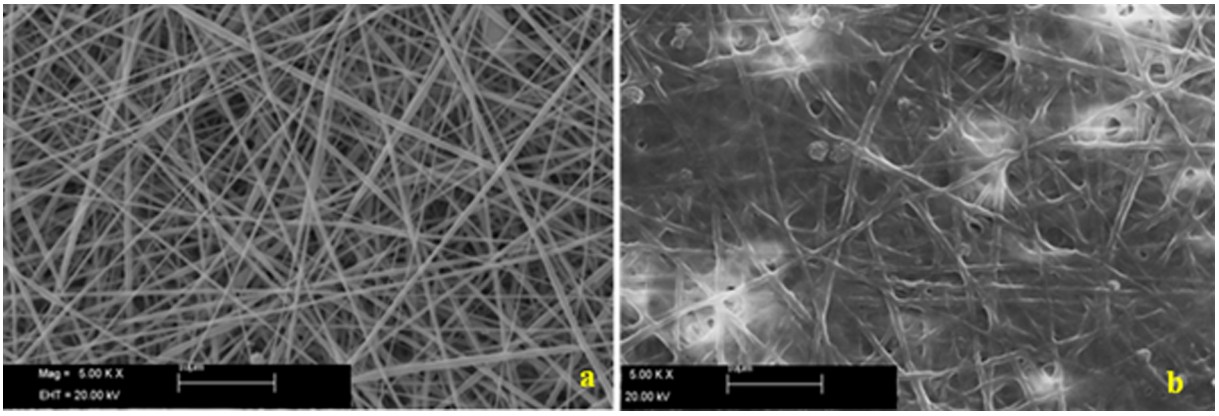

Fig. 12. SEM images of NFM 6 membranes (a) before BSA filtration and (b) after BSA filtration.

that the fabricated PSF NFM membranes were loose UF membranes [42,43].

In Fig. 12, SEM images of NFM6 before and after BSA filtration were given. As shown in Fig. 12, rejected BSA can be clearly observed on the surface of NFM6 membrane. According to the literature, the BSA fouling can be developed in both microfiltration and ultrafiltration. In this study as supported by the literature [63,64] the filtering of BSA could be explained by two main mechanisms; (i) the retention of proteins aggregates or the adsorption of BSA on the surface of the membranes. During the filtration process, fouling mainly occurred along the surface of the electrospun membrane since particles were mostly retained on the membrane surface, (ii) the chemical attachment of BSA to the protein aggregates.

4. Conclusions

In the present research, a novel hydrophilic and mechanically robust PSF nanofiber membrane was obtained by electrospinning the PSF solution blended with different ratios of PEI and Al_2O_3 nanoparticles without any support for using in water based membrane filtration applications. The incorporation of PEI and Al_2O_3 improved the overall properties of the nanofiber membranes in terms of porosity, tensile strength and hydrophilicity depended on the loading amount of PEI and Al_2O_3. Although the PSF NFMs containing increasing amounts of PEI were exhibited better characteristics in terms of pure water flux and BSA rejection compared to the PSF NFM, PSF/PEI-Al_2O_3 nanofiber membranes relatively have an excellent characteristic with the increasing amount of nanoparticles. The results showed that after blending the PSF solution with 2 wt.% PEI and 0.05 wt.% Al_2O_3, subsequent electrospinning led to improving the hydrophilicity of the NFMs, and therefore increased the pure water flux and the rejection performance of the PSF nanofiber membranes. Also, the tensile strength was improved at higher PEI and Al_2O_3 amount by 140% and 360% from 0.1 MPa to 0.3 and 0.6 MPa, respectively. From the above results, it is inferred that additive combined PSF/PEI-Al_2O_3 nanofiber membranes have better characteristic membrane properties and higher BSA rejection. Overall, this research indicates that a promising potential for further evaluation of NFMs with incorporation additives such as PEI and Al_2O_3 and they can be used to improved mechanical strength which will also enhance prospects for handling without the need of an additional support.

Acknowledgement

The authors extend their appreciation to the Scientific Research Foundation of Abdullah Gül University (Project No. FYL-2016) for funding this study.

References

[1] S. Ramakrishna, R. Jose, P.S. Archana, A.S. Nair, R. Balamurugan, J. Venugopal, W.E. Teo, Science and engineering of electrospun nanofibers for advances in clean energy, water filtration, and regenerative medicine, J. Mater. Sci. 45 (2010) 6283–6312.
[2] S. Ramakrishna, K. Fujihara, W.-E. Teo, T.-C. Lim, Z. Ma, An Introduction to Electrospinning and Nanofibers, World Scientific, 2005.
[3] K. Yoon, B.S. Hsiao, B. Chu, Functional nanofibers for environmental applications, J. Mater. Chem. 18 (2008) 5326–5334.
[4] S. Agarwal, A. Greiner, J.H. Wendorff, Functional materials by electrospinning of polymers, Prog. Polym. Sci. 38 (2013) 963–991.
[5] Z. Ma, M. Kotaki, S. Ramakrishna, Electrospun cellulose nanofiber as affinity membrane, J. Membr. Sci. 265 (2005) 115–123.
[6] R. Gopal, S. Kaur, C.Y. Feng, C. Chan, S. Ramakrishna, S. Tabe, T. Matsuura, Electrospun nanofibrous polysulfone membranes as pre-filters: particulate removal, J. Membr. Sci. 289 (2007) 210–219.
[7] C. Feng, K.C. Khulbe, T. Matsuura, S. Tabe, A.F. Ismail, Preparation and characterization of electro-spun nanofiber membranes and their possible applications in water treatment, Sep. Purif. Technol. 102 (2013) 118–135.
[8] S.A.A.N. Nasreen, S. Sundarrajan, S.A.S. Nizar, R. Balamurugan, S. Ramakrishna, Advancement in electrospun nanofibrous membranes modification and their application in water treatment, Membranes 3 (2013) 266–284.
[9] M. Essalhi, M. Khayet, Self-sustained webs of polyvinylidene fluoride electrospun nanofibers at different electrospinning times: 1. Desalination by direct contact membrane distillation, J. Membr. Sci. 433 (2013) 167–179.
[10] S. Kiani, S. Mousavi, N. Shahtahmassebi, E. Saljoughi, Preparation and characterization of polyphenylsulfone nanofibrous membranes for the potential use in liquid filtration, Desalin. Water Treat. 57 (2016) 16250–16259.
[11] A. Bazargan, M. Keyanpour-Rad, F. Hesari, M.E. Ganji, A study on the microfiltration behavior of self-supporting electrospun nanofibrous membrane in water using an optical particle counter, Desalination 265 (2011) 148–152.
[12] K. Yoon, B.S. Hsiao, B. Chu, High flux ultrafiltration nanofibrous membranes based on polyacrylonitrile electrospun scaffolds and crosslinked polyvinyl alcohol coating, J. Membr. Sci. 338 (2009) 145–152.
[13] K. Yoon, B.S. Hsiao, B. Chu, High flux nanofiltration membranes based on interfacially polymerized polyamide barrier layer on polyacrylonitrile nanofibrous scaffolds, J. Membr. Sci. 326 (2009) 484–492.
[14] J. Xu, N. Cai, W. Xu, Y. Xue, Z. Wang, Q. Dai, F. Yu, Mechanical enhancement of nanofibrous scaffolds through polyelectrolyte complexation, Nanotechnology 24 (2012) 025701.
[15] A. Baji, Y.-W. Mai, S.-C. Wong, M. Abtahi, P. Chen, Electrospinning of polymer nanofibers: effects on oriented morphology, structures and tensile properties, Compos. Sci. Technol. 70 (2010) 703–718.
[16] T.D. Brown, P.D. Dalton, D.W. Hutmacher, Melt electrospinning today: an opportune time for an emerging polymer process, Prog. Polym. Sci. 56 (2016) 116–166.
[17] G. Kim, R. Lach, G. Michler, P. Pötschke, K. Albrecht, Relationships between phase morphology and deformation mechanisms in polymer nanocomposite nanofibres prepared by an electrospinning process, Nanotechnology 17 (2006) 963.
[18] A. Lee, J.W. Elam, S.B. Darling, Membrane materials for water purification: design, development, and application, Environ. Sci. Water Res. Technol. 2 (2016) 17–42.
[19] K.C. Khulbe, T. Matsuura, Recent progress in polymeric hollow-fibre membrane preparation and applications, Membr. Technol. 2016 (2016) 7–13.
[20] J.R. Werber, C.O. Osuji, M. Elimelech, Materials for next-generation desalination and water purification membranes, Nat. Rev. Mater. 1 (2016) 16018.
[21] F. Mahmoudi, E. Saljoughi, S.M. Mousavi, Promotion of polysulfone membrane by thermal-mechanical stretching process, J. Polym. Res. 20 (2013) 1–10.

[22] S. Zhao, Z. Wang, X. Wei, B. Zhao, J. Wang, S. Yang, S. Wang, Performance improvement of polysulfone ultrafiltration membrane using PANiEB as both pore forming agent and hydrophilic modifier, J. Membr. Sci. 385 (2011) 251–262.
[23] N. Sharma, M. Purkait, Enantiomeric and racemic effect of tartaric acid on polysulfone membrane during crystal violet dye removal by MEUF process, J. Water Process Eng. 10 (2016) 104–112.
[24] A.K. Nair, P. Shalin, P. JagadeeshBabu, Performance enhancement of polysulfone ultrafiltration membrane using TiO_2 nanofibers, Desalin. Water Treat. 57 (2016) 10506–10514.
[25] E. Eren, A. Sarihan, B. Eren, H. Gumus, F.O. Kocak, Preparation, characterization and performance enhancement of polysulfone ultrafiltration membrane using PBI as hydrophilic modifier, J. Membr. Sci. 475 (2015) 1–8.
[26] W.-E. Teo, S. Ramakrishna, Electrospun nanofibers as a platform for multifunctional, hierarchically organized nanocomposite, Compos. Sci. Technol. 69 (2009) 1804–1817.
[27] S. Jiang, L.-P. Lv, K. Landfester, D. Crespy, Nanocontainers in and onto nanofibers, Acc. Chem. Res. (2016).
[28] M. Baghbanzadeh, D. Rana, C.Q. Lan, T. Matsuura, Effects of inorganic nano-additives on properties and performance of polymeric membranes in water treatment, Sep. Purif. Rev. 45 (2016) 141–167.
[29] L. Jin, S. Yu, W. Shi, X. Yi, N. Sun, Y. Ge, C. Ma, Synthesis of a novel composite nanofiltration membrane incorporated SiO_2 nanoparticles for oily wastewater desalination, Polymer 53 (2012) 5295–5303.
[30] Y. Teow, A. Ahmad, J. Lim, B. Ooi, Preparation and characterization of PVDF/TiO_2 mixed matrix membrane via in situ colloidal precipitation method, Desalination 295 (2012) 61–69.
[31] U. Habiba, A.M. Afifi, A. Salleh, B.C. Ang, Chitosan/(polyvinyl alcohol)/zeolite electrospun composite nanofibrous membrane for adsorption of Cr^{6+}, Fe^{3+} and Ni^{2+}, J. Hazard. Mater. 322 (2016) 182–194.
[32] Y. Medina-Gonzalez, J.-C. Remigy, Sonication-assisted preparation of pristine MWCNT–polysulfone conductive microporous membranes, Mater. Lett. 65 (2011) 229–232.
[33] Y. Zhang, L. Wang, Y. Xu, ZrO_2 solid superacid porous shell/void/TiO_2 core particles (ZVT)/polyvinylidene fluoride (PVDF) composite membranes with anti-fouling performance for sewage treatment, Chem. Eng. J. 260 (2015) 258–268.
[34] X. Zhang, Y. Wang, Y. Liu, J. Xu, Y. Han, X. Xu, Preparation, performances of PVDF/ZnO hybrid membranes and their applications in the removal of copper ions, Appl. Surf. Sci. 316 (2014) 333–340.
[35] L. Yan, Y.S. Li, C.B. Xiang, S. Xianda, Effect of nano-sized Al_2O_3-particle addition on PVDF ultrafiltration membrane performance, J. Membr. Sci. 276 (2006) 162–167.
[36] J. Garcia-Ivars, M.-I. Alcaina-Miranda, M.-I. Iborra-Clar, J.-A. Mendoza-Roca, L. Pastor-Alcañiz, Enhancement in hydrophilicity of different polymer phase-inversion ultrafiltration membranes by introducing PEG/Al_2O_3 nanoparticles, Sep. Purif. Technol. 128 (2014) 45–57.
[37] J. Dai, K. Xiao, H. Dong, W. Liao, X. Tang, Z. Zhang, S. Cai, Preparation of Al_2O_3/PU/PVDF composite membrane and performance comparison with PVDF membrane, PU/PVDF blending membrane, and Al_2O_3/PVDF hybrid membrane, Desalin. Water Treat. 57 (2016) 487–494.
[38] H. Dong, K.-J. Xiao, X.-L. Li, Z.-M. Wang, Stability of nano-Al_2O_3 Sol and properties of PVDF/Al_2O_3 hybrid membrane, J. Mod. Food Sci. Technol. 12 (2012) 002.
[39] F. Liu, M.M. Abed, K. Li, Preparation and characterization of poly (vinylidene fluoride)(PVDF) based ultrafiltration membranes using nano γ-Al_2O_3, J. Membr. Sci. 366 (2011) 97–103.
[40] H. Basri, A.F. Ismail, M. Aziz, Polyethersulfone (PES)–silver composite UF membrane: effect of silver loading and PVP molecular weight on membrane morphology and antibacterial activity, Desalination 273 (2011) 72–80.
[41] S.-J. Park, R.K. Cheedrala, M.S. Diallo, C. Kim, I.S. Kim, W.A. Goddard III, Nanofiltration membranes based on polyvinylidene fluoride nanofibrous scaffolds and crosslinked polyethyleneimine networks, J. Nanopart. Res. 14 (2012) 1–14.
[42] F. Geng, L. Zheng, L. Yua, G. Li, C. Tung, Interaction of bovine serum albumin and long-chain imidazolium ionic liquid measured by fluorescence spectra and surface tension, Process Biochem. 45 (2010) 306–311.
[43] J. Qi, P. Yao, F. He, C. Yu, C. Huang, Nanoparticles with dextran/chitosan shell and BSA/chitosan core—doxorubicin loading and delivery, Int. J. Pharm. 393 (2010) 176–184.
[44] Z. Zhao, J. Zheng, M. Wang, H. Zhang, C.C. Han, High performance ultrafiltration membrane based on modified chitosan coating and electrospun nanofibrous PVDF scaffolds, J. Membr. Sci. 394 (2012) 209–217.
[45] S. Mallakpour, M. Dinari, Enhancement in thermal properties of poly(vinyl alcohol) nanocomposites reinforced with Al_2O_3 nanoparticles, J. Reinf. Plast. Compos. 32 (2013) 217–224.
[46] W. Cui, X. Li, S. Zhou, J. Weng, Degradation patterns and surface wettability of electrospun fibrous mats, Polym. Degrad. Stab. 93 (2008) 731–738.
[47] M. Obaid, G.M. Tolba, M. Motlak, O.A. Fadali, K.A. Khalil, A.A. Almajid, B. Kim, N.A. Barakat, Effective polysulfone-amorphous SiO_2 NPs electrospun nanofiber membrane for high flux oil/water separation, Chem. Eng. J. 279 (2015) 631–638.
[48] M.R. Johan, O.H. Shy, S. Ibrahim, S.M. Mohd Yassin, T.Y. Hui, Effects of Al_2O_3 nanofiller and EC plasticizer on the ionic conductivity enhancement of solid PEO-LiCF3SO3 solid polymer electrolyte, Solid State Ionics 196 (2011) 41–47.
[49] C.C. Yang, SJ. Chiu, WC Chien, SS Chiu, Quaternized poly(vinyl alco-hol)/alumina composite polymer membranes for alkaline direct methanol fuel cells, J. Power Sources 195 (2010) 2212–2219.
[50] W. Zhou, S. Qi, C. Tu, H. Zhao, C. Wang, J. Kou, Effect of the particle size of Al_2O_3 on the properties of filled heat-conductive silicone rubber, J. Appl Polym. Sci. 104 (2007) 1312–1318.
[51] S. Zhang, X.Y. Cao, Y.M. Ma, Y.C. Ke, J.K. Zhang, F.S. Wang, The effects of particle size and content on the thermal conductivity and mechanical properties of Al_2O_3/high density polyethylene (HDPE) composites, Exp. Polym. Lett. 5 (2011) 581–590.
[52] S.S. Homaeigohar, M. Elbahri, Novel compaction resistant and ductile nanocomposite nanofibrous microfiltration membranes, J. Colloid Interface Sci. 372 (2012) 6–15.
[53] H. Hou, J.J. Ge, J. Zeng, Q. Li, D.H. Reneker, A. Greiner, S.Z. Cheng, Electrospun polyacrylonitrile nanofibers containing a high concentration of well-aligned multiwall carbon nanotubes, Chem. Mater. 17 (2005) 967–973.
[54] Z. Ma, M. Kotaki, S. Ramakrishna, Surface modified nonwoven polysulphone (PSU) fiber mesh by electrospinning: a novel affinity membrane, J. Membr. Sci. 272 (2006) 179–187.
[55] L. Huang, S.S. Manickam, J.R. McCutcheon, Increasing strength of electrospun nanofiber membranes for water filtration using solvent vapor, J. Membr. Sci. 436 (2013) 213–220.
[56] Zi Xu, X. Li, K.Teng, B. Zhou, M. Ma, M. Shan, K. Jiao, X. Qian, J. Fan, High flux and rejection of hierarchical composite membranes based on carbon nanotube network and ultrathin electrospun nanofibrous layer for dye removal, J. Membr. Sci. 535 (2017) 94–102
[57] A.D. Kiadehi, A. Rahimpour, M. Jahanshahi, A.A. Ghoreyshi, Novel carbon nano-fibers (CNF)/polysulfone (PSF) mixed matrix membranes for gas separation, J. Ind. Eng. Chem. 22 (2015) 199–207.
[58] N.N. Rupiasih, H. Suyanto, M. Sumadiyasa, N. Wendri, Study of effects of low doses UV radiation on microporous polysulfone membranes in sterilization process, J. Org. Polym. Mater. 3 (2013) 12–18.
[59] H. Dong, K.-J. Xiao, X.-L. Li, Y. Ren, S.-Y. Guo, Preparation of PVDF/Al_2O_3 hybrid membrane via the sol–gel process and characterization of the hybrid membrane, Desalin. Water Treat. 51 (2013) 3685–3690.
[60] S. Kiani, S.M. Mousavi, N. Shahtahmassebi, E. Saljoughi, Hydrophilicity improvement in polyphenylsulfone nanofibrous filtration membranes through addition of polyethylene glycol, Appl. Surf. Sci. 359 (2015) 252–258.
[61] S. Guclu, M.E. Pasaoglu, I. Koyuncu, Membrane manufacturing via simultaneous electrospinning of PAN and PSU solutions, Desalin. Water Treat. 57 (2016) 8152–8160.
[62] L.A. Goetz, B. Jalvo, R. Rosal, A.P. Mathew, Superhydrophilic anti-fouling electrospun cellulose acetate membranes coated with chitin nanocrystals for water filtration, J. Membr. Sci. 510 (2016) 238–248.
[63] S.T. Kelly, A.L. Zydney, Mechanisms for BSA fouling during microfiltration, J. Membr. Sci. 107 (1995) 115–127.
[64] H. Esfahani, M.P. Prabhakaran, E. Salahi, A. Tayebifard, M.R. Rahimipour, M. Keyanpour-Rad, S. Ramakrishna, Electrospun nylon 6/zinc doped hydroxyapatite membrane for protein separation: mechanism of fouling and blocking model, Mater. Sci. Eng. C 59 (2016) 420–428.